J. Indian Chem. Soc.,
Vol. 89, August 2012, pp. 1071-1084

The reaction of heterocyclic amine with pendant naphthyl group in $Pd(\alpha/\beta\text{-NaiR})Cl_2$ (α/β-NaiR = 1-alkyl-2-(naphthyl-α/β-azo)imidazoles) and the product characterisation†

Pampa Pratihar[a], Paramita Dutta[a], Papia Datta[a], Dibakar Sardar[a], A. M. Z. Slawin[b] and C. Sinha[a]*

[a]Department of Chemistry, Inorganic Chemistry Section, Jadavpur University, Kolkata-700 032, India

E-mail : c_r_sinha@yahoo.com

[b]Department of Chemistry, University of St-Andrews, St-Andrews, KY16 9ST, UK

Manuscript received 06 February 2012, accepted 10 February 2011

Abstract : The reaction of $Pd(\alpha/\beta\text{-NaiR})Cl_2$ (1-alkyl-2-(naphthyl-α/β-azo)imidazoles, α-NaiR (1) and β-NaiR (2)) with *m*-aminopyridine (*m*-NH_2-Py) and *o*-aminopyrimidine (*o*-NH_2-Pym) in acetonitrile solution has synthesized a C–N coupled product, chloro[1-alkyl-2-{(7-imidophenyl)pyridyl-α/β-azo}imidazole-N,N′,N″]palladium(II), $Pd(\alpha/\beta\text{-NaiR-N-Py-}m)Cl$ (3, 4) and $Pd(\alpha/\beta\text{-NaiR-}N_2\text{-Py-}o)Cl$ (5, 6). The structural confirmation has been carried out by X-ray diffraction study. The solution electronic spectra of C–N fused products, 3-6, show transitions within 600–900 nm those are absent in $Pd(\alpha/\beta\text{-NaiR})Cl_2$. Cyclic voltammogram shows four successive redox couples, one of them (positive to SCE) is oxidative in nature and others (negative to SCE) are ligand reductions. Emission is observed from ligand centred orbitals and has been ascribed to π-π* excitation process. The excited state decays following radiative and nonradiative biexponential routes. Absorption and fluorescence spectra of pyridylamine fusion product show H^+ and metal ion (Zn^{2+}, Cd^{2+}) sensitivity.

Keywords : Pd-naphthylazoimidazoles, C–N coupling reaction, LLCT, electrochemistry, luminescence, H^+-sensitivity.

Introduction

The C–H activation is highly acclaimed in the synthetic chemistry. A significant progress has been achieved in this area by using metal catalysed route. Facile C–H activation and formation of organometallic compounds, and the subsequent reactions of the metal-carbon bonded motif which could not be observed otherwise[6–8] is a fascinating field of chemical research. The transition metal complex of azo ligands is a field of research interest for fascinating electron transfer[1–4], photophysical[5] behaviour of delocalised metallated chelates of bi- and tridentate ligands and metal assisted organic transformation of chelated ligand to a new molecule which is otherwise impossible to synthesise[7–10]. It is observed that the pendant aromatic ring in metallated azo-heterocycles does not fit to chelate with central metal ion because of ring strain (in four member ring) but efficiently activate *ortho* C–H bond followed by hydroxylation[9], thiolation[10] or amine coupling reaction[7,8]. Free ligands do not show such chemical reactions. The N(1)-substituted 2-(arylazo)imidazole ligands have been extensively investigated in our laboratory in recent years[3,11–15]. In particular, we have reported the synthesis, spectroscopic studies and structural characterisation of Pd^{II} compounds with N(1)-alkyl-2-(arylazo)imidazoles[15]. These classes of molecules carry azoimine, -N=N–C=N-, group. They are π-deficient and stabilize low valent metal redox state. The coordination of ligand(s) with metal ion can offer suitable orientations and electronic requirement for participation in chemical reactions. In the metal promoted organic reactions[7–10] the transition metal ions serve as effective template.

We have initiated a research programme on palladium(II)-mediated C–N coupling reaction of coordinated 1-alkyl-2-(naphthyl-α/β-azo)imidazoles by using aromatic and heterocyclic amines[16]. In this work we will report the C–N fusion of $Pd(\alpha/\beta\text{-NaiR})Cl_2$ (α-NaiR = 1-alkyl-2-(naphthyl-α-azo)imidazoles); β-NaiR = 1-alkyl-2-(naphthyl-β-azo)imidazoles)) with *m*-aminopyridine (*m*-NH_2Py)

†In honour of Professor K. B. Pandeya on the occasion of his 70th Birth Anniversary.

and *o*-aminopyrimidine (*o*-NH_2Pym). The complexes have been characterized by the spectral, electrochemical and luminescence data. The structural confirmation has been established by single crystal X-ray diffraction studies. These complexes show polarity dependent absorption and emission properties in different solvents. The spectral and redox properties are explained by DFT and TD-DFT calculations.

Results and discussion

Synthesis and formulation :

Dichloro-(1-alkyl-2-(naphthyl-α/β-azo)imidazole)-palladium(II) complexes, Pd(α-NaiR)Cl_2 (**1**), Pd(β-NaiR)Cl_2 (**2**) are used in this work. The reaction between Pd(α/β-NaiR)Cl_2, *m*-NH_2Py or *o*-NH_2Pym (1 : 1.4 molar ratio) in presence of Et_3N in MeCN solution under stirring and refluxing for 10 h has yielded green product (eq. (1)). This has been identified as amine coupled product [Pd(α/β-NaiR-N-C_5H_4N-*m*)Cl] (**3**, **4**) and [Pd(α/β-NaiR-N-$C_5H_3N_2$-*o*)Cl] (**5**, **6**) [where, R = CH_3 (**a**), CH_2CH_3 (**b**), CH_2Ph (**c**); α-derivatives are **3**, **5** and β-derivatives are **4**, **6**)].

The C–N coupling takes place by the C–H activation of *ortho* C(6)–H bond to the azo function in the pendant naphthyl ring (**B**-ring) of NaiR and forms palladium(II) complex of tridentate N,N′,N″-chelating ligand (N, N′, N″ refer to N(imidazole), N(azo) and N(pyridylamine) respectively). Microanalytical data support the composition of the complexes (see Experimental section). There is a feasibility of C(8)–H activation; the proximate position of C(9)–H may prevent the fusion at C(8) position.

Molecular structures :

The molecular structures of Pd(α-NaiEt-N-C_5H_4N-*m*)Cl (**3b**) and Pd(α-NaiMe-N-$C_4H_3N_2$-*o*)Cl (**5a**) are shown in Figs. 1 and 2. The selected bond parameters are listed in Table 1. The asymmetric unit of **3b** crystal lattice consists of one molecule while that of **5a** is constituted of two molecules. Each molecular unit of the structure shows tridendate N(imidazole) (N), N(azo) (N′), N(amine) (N″) coordination of the chelating ligand and fourth coordination site of the square plane is occupied by -Cl··· There are two chelate rings; the atomic groups Pd(1), N(1), C(2), N(6), N(7) and Pd(1), N(7), C(8),

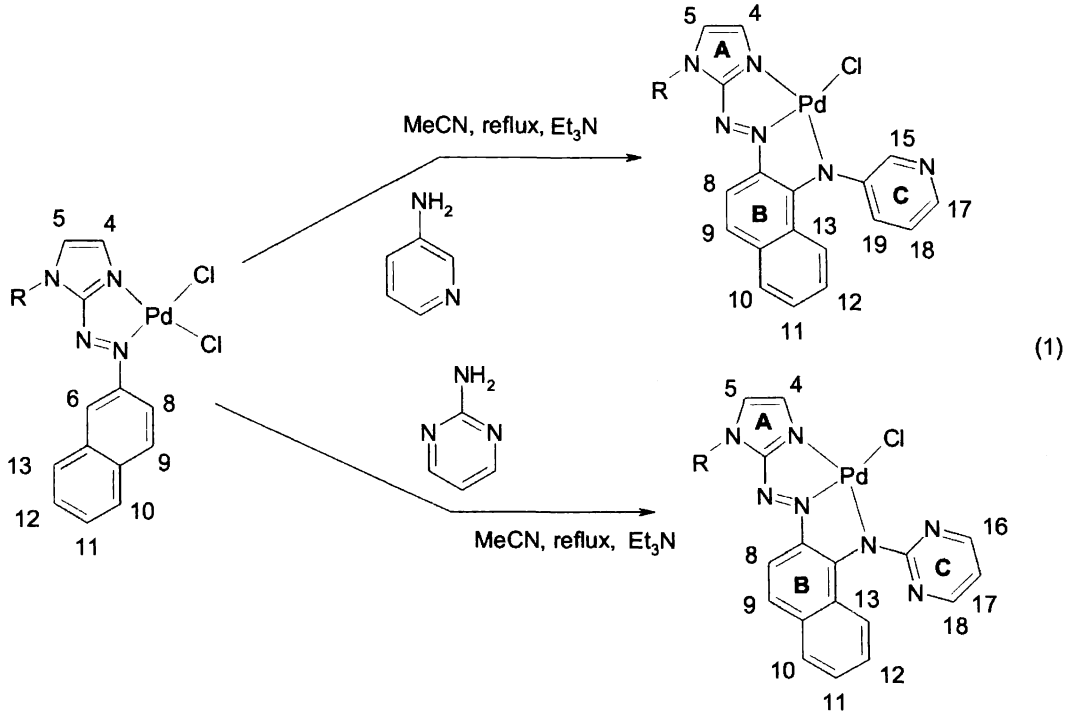

Scheme 1. C–N fusion reaction. Pd(α-NaiR)Cl_2 (**1**), Pd(β-NaiR)Cl_2 (**2**); Pd(α-NaiR-N-C_5H_4N-*m*)Cl (**3**); Pd(β-NaiR-N-C_5H_4N-*m*)Cl (**4**); [Pd(α-NaiR-N-$C_5H_3N_2$-*o*)Cl] (**5**); [Pd(β-NaiR-N-$C_5H_3N_2$-*o*)Cl] (**6**) and R = CH_3 (**a**), CH_2CH_3 (**b**), CH_2Ph (**c**).

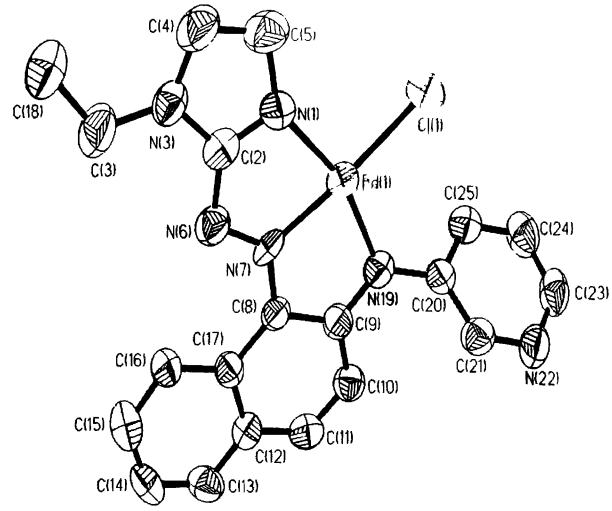

(a)

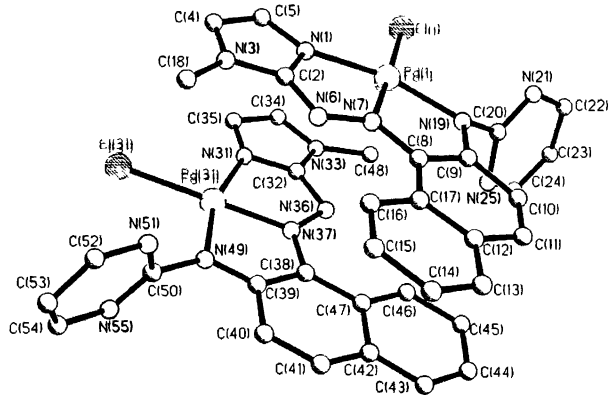

(b)

Fig. 1. Molecular structure of (a) Pd(α-NaiEt-N-C_5H_4N-*m*)Cl (**3b**) and (b) Pd(α-NaiMe-N-$C_4H_3N_2$-*o*)Cl (**5a**).

C(9), N(19) [Pd(31), N(31), C(32), N(36), N(37) and Pd(31), N(37), C(38), C(39), N(49)] constitute two chelate planes (mean deviation, < 0.04 Å) and they are nearly planar (dihedral angle 4°). The chelate bite angles are N(1)-Pd(1)-N(7), 80.1(2)° (**3b**), 79.5(3), (N(37)-Pd(31)-N(31), 80.9(4)°) (**5a**) and N(7)-Pd(1)-N(19), 80.6(2)° (**3b**) and 81.2(3) (N(37)-Pd(31)-N(49), 81.6(4)°) (**5a**). The Pd atom lies within the square plane defined by N_3Cl donor centers (deviation, < 0.01). The pendant heterocycle ring is inclined at an angle of 22.14° (**3b**) and 23.18° (**5a**) with the principal plane. There are three types of Pd-N bonds : Pd–N(imidazole) [Pd(1)-N(1)], 2.030(6) (**3b**), 2.009(7) (**5a**) and Pd(31)–N(31), 2.030(9) Å (isomer of **5a**)]; Pd-N(azo) [Pd(1)-N(7)], 1.939(6) (**3b**), 1.954(7) (**5a**) and Pd(31)–N(37), 1.934(9) Å (isomer of **5a**)] and Pd-N(heterocycle), Pd(1)-N(19), 2.026(6) (**3b**), 1.998(8) (**5a**) and Pd(31)–N(49), 2.009(9) Å (isomer of **5a**). These distances are within limits of reported data[15]. The N=N bond lengths are N(6)–N(7), 1.328(7) (**3b**); 1.309(9) (**5a**) and N(36)-N(37), 1.331(12) Å (isomer of **5a**). The free ligand value of N=N bond is 1.267(3) Å available for 1-ethyl-2-(naphthyl-α-azo)imidazolium hexafluorophosphate[27]. The elongation of N=N distance is consistent with electron delocalization from metal to ligand fragment. The difference in N(azo)-C(naphthyl-B/imidazole-A) may be due to backbone conjugation in the coordinated anionic ligand. The N(azo)-C(imidazole-A) (N(6)-C(2)), 1.386(10) (**3b**), 1.363(12) (**5a**) and 1.388(14) Å (isomer **5a**); N(azo)-C(naphthyl-B) (N(7)-C(8)) 1.364(8)

Table 1. Selected bond length (Å) and angles (°) of Pd(α-NaiEt-N-C_5H_4N-*m*)Cl (**3b**) Pd(α-NaiMe-N-$C_4H_3N_2$-*o*)Cl (**5a**)

Pd(1)-N(1)	2.009(7)	N(7)-Pd(1)-N(1)	79.5(3)
Pd(1)-N(7)	1.954(7)	N(7)-Pd(1)-N(19)	81.2(3)
Pd(1)-N(19)	1.998(8)	N(19)-Pd(1)-N(1)	160 6(3)
Pd(1)-Cl(1)	2.298(3)	N(7)-Pd(1)-Cl(1)	177.7(2)
N(6)-N(7)	1.309(9)	N(19)-Pd(1)-Cl(1)	100.8(2)
N(7)-C(8)	1.369(11)	N(1)-Pd(1)-Cl(1)	98.6(3)
C(9)-N(19)	1.338(13)	C(2)-N(1)-Pd(1)	108.3(7)
N(19)-C(20)	1.405(14)	C(5)-N(1)-Pd(1)	144.2(7)
C(2)-N(6)	1.363(12)	N(6)-N(7)-Pd(1)	119 7(6)
C(2)-N(6)	1.363(12)	N(6)-N(7)-Pd(1)	119.7(6)
C(8)-C(9)	1.441(12)	C(8)-N(7)-Pd(1)	116.3(6)

Table-1 (contd.)

Pd(α-NaiEt-N-C_5H_4N-*m*)Cl (**3b**)			
Pd(1)-N(1)	2.030(6)	N(7)-Pd(1)-N(1)	80.1(2)
Pd(1)-N(7)	1.939(6)	N(7)-Pd(1)-N(19)	80.6(2)
Pd(1)-N(19)	2.026(6)	N(19)-Pd(1)-N(1)	160.6(2)
Pd(1)-Cl(1)	2.304(2)	N(7)-Pd(1)-Cl(1)	175.45(16)
N(6)-N(7)	1.328(7)	N(19)-Pd(1)-Cl(1)	102.83(18)
N(7)-C(8)	1.364(8)	N(1)-Pd(1)-Cl(1)	96.60(18)
C(9)-N(19)	1.336(9)	C(2)-N(1)-Pd(1)	107.0(5)
N(19)-C(20)	1.430(9)	C(5)-N(1)-Pd(1)	145.2(6)
C(2)-N(6)	1.386(10)	N(6)-N(7)-Pd(1)	120.1(4)
C(8)-C(9)	1.444(9)	C(8)-N(7)-Pd(1)	118.2(4)

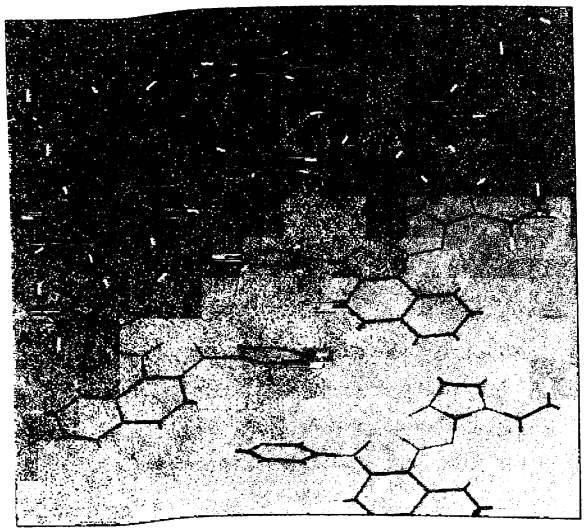

(a)

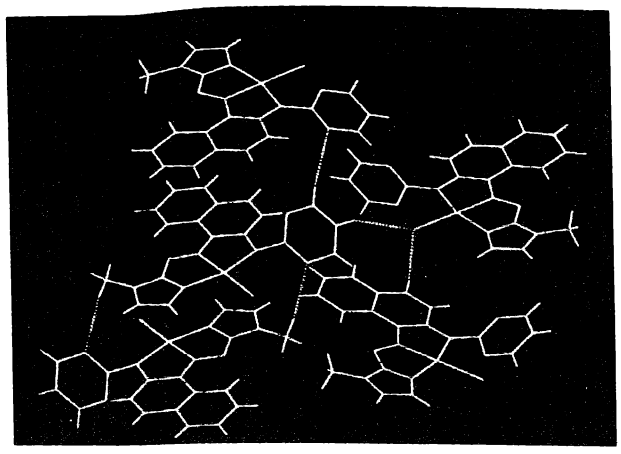

(b)

Fig. 2. Hydrogen bonding network in (a) **3b** and (b) **5a**.

(**3b**), 1.369(11) (**5a**) and 1.392(14) Å (isomer of **5a**) are noticeably shorter than that of N(imino)-C(heterocycle) (N(19)-C(20)), 1.430(9) in **3b**, 1.405(14) (**5a**) and N(49)-C(50), 1.447(15) Å.

Hydrogen bonded 1D chain is observed in **3b** through C(10)–H(10)---N(22A) (C(10)–H(10), 0.95 Å; H(10)---N(22A), 2.69(4) Å; C(10)---N(22A), 3.45(3) Å and ∠C(10)–H(10)---N(22A), 137.3(6)°) and C(24)–H(24)---Cl(1) (C(24)–H(24), 0.95 Å; H(24)---Cl(1A), 2.75(9) Å; C(24)---Cl(1A), 3.61(5) Å and ∠C(24)–H(24)---Cl(1A), 150.3(2)°) (Fig. 2a). In **5a** the Cl of Pd–Cl bond shows bifurcated hydrogen bonds (Fig. 2b) with naphthyl-H (C(41)–H(41A)---Cl(31) : C---Cl, 3.64(2); H---Cl, 2.75(7); ∠C(41)–H(41A)---Cl(31), 155.2(8)°) and pyrimidyl-H (C(23)–H(23A)---Cl(31) : C---Cl, 3.48(7); H---Cl, 2.63(7); ∠C(23)–H(23A)---Cl(31), 48.9(6)°). Pyrimidine-N of one molecule contacts neighbouring molecules through hydrogen bonds with C–H of pyrimidine-H (C(24)–H(24A)---N(55) : C---N, 3.59(8); H---N, 2.68(3); ∠C(24)–H(24A)---N(55), 161.7(3)°) and H of N-CH_3 in imidazolyl motif (C(18)–H(18A)---N(21) : C---N, 3.49(5); H---N, 2.57(5); ∠C(18)–H(18A)---N(21), 156.2(1)°).

Spectral studies :

IR spectra :

Main difference in infra-red spectra is the presence of one ν(Pd–Cl) stretch at 320 cm^{-1} in Pd(α/β-NaiR-N-C_5H_4N-*m*)Cl (**3**, **4**) and Pd(α/β-NaiR-N-$C_4H_3N_2$-*o*)Cl (**5**, **6**) compared to two ν(Pd–Cl) stretches at 330 and 310 cm^{-1} [9,15] of precursor Pd(α/β-NaiR)Cl_2. The sharp single band at 1335–1350 cm^{-1} in **3-6** is referred to ν(N=N) which has been shifted to lower frequency by 15–20 cm^{-1} compared to free ligand data and by 10–15 cm^{-1} from that of Pd(α/β-NaiR)Cl_2. This supports the coordination of

Table 2. UV-Vis and emission spectral data of Pd(α/β-NaiR-N-C_5H_4N-*m*)Cl and Pd(α/β-NaiR-N-$C_4H_3N_2$-*o*)Cl in MeCN

Complexes	λ_{max}/nm (10^{-3} ε [dm^3 mol^{-1} cm^{-1}])[a]	λ_{ex}/nm[b]	λ_{em}/nm[c]	Φ_f
Pd(α-NaiMe-N-C_5H_4N-*m*)Cl (**3a**)	220(10.01), 241(8.20), 306(4.98), 397(8.21), 417(8.62), 704(0.20), 776(0.15), 851(0.11)	306	349	0.04
Pd(α-NaiEt-N-C_5H_4N-*m*)Cl (**3b**)	253(10.88), 308(5.23), 349(4.83), 415(2.11), 474(1.39), 713(1.88), 773(2.36), 852(1.68)	253	372	0.02
Pd(α-NaiBz-N-C_5H_4N-*m*)Cl (**3c**)	240(12.14), 333(8.45), 399(14.41), 418(13.68), 644(0.23), 711(0.38), 775(0.43), 852(0.29)	333	361	0.01
Pd(β-NaiMe-N-C_5H_4N-*m*)Cl (**4a**)	287(10.24), 298(9.55), 376(5.83), 395(3.38), 641(0.71), 701(0.12), 807(0.21), 850(0.15)	298	365	0.02
Pd(β-NaiEt-N-C_5H_4N-*m*)Cl (**4b**)	286(4.19), 300(4.05), 380(9.54), 396(7.46), 423(3.97), 479(1.38), 639(0.21), 703(0.46), 807(0.56), 842(0.43)	300	360	0.03
Pd(β-NaiBz-N-C_5H_4N-*m*)Cl (**4c**)	293(4.20), 370(4.06), 642(0.19), 698(0.28), 801(0.21), 855(0.17)	293	405	0.06
Pd(α-NaiMe-N-$C_4H_3N_2$-*o*)Cl (**5a**)	259(11.12), 409(8.19), 573(1.67), 540(0.61), 699(0.84), 749(0.80), 828(0.60)	259	368	0.14
Pd(α-NaiEt-N-$C_4H_3N_2$-*o*)Cl (**5b**)	273(6.45), 332(4.92), 399(7.97), 415(7.55), 448(4.29), 503(1.68), 708(0.13), 820(0.30)	332	431	0.09
Pd(α-NaiBz-N-$C_4H_3N_2$-*o*)Cl (**5c**)	269(7.75), 402(11.03), 418(10.67), 644(0.33), 707(0.34), 816(0.34)	269	339	0.11
Pd(β-NaiMe-N-$C_4H_3N_2$-*o*)Cl (**6a**)	253(10.02), 395(6.72), 540(1.54), 642(0.50), 675(0.75), 740(0.89), 832(0.40)	253	371	0.11
Pd(β-NaiEt-N-$C_4H_3N_2$-*o*)Cl (**6b**)	282(5.43), 340(5.21), 381(6.01), 470(3.25), 514(2.03), 712(0.11), 825(0.25)	282	375	0.13
Pd(β-NaiBz-N-$C_4H_3N_2$-*o*)Cl (**6c**)	215(10.97), 265(14.12), 285(10.68), 297(9.01), 381(23.26), 512(4.09), 654(0.15), 718(0.11), 821(0.21)	285	378	0.16

[a]Solvent : MeCN; [b]λ_{ex} - excitation wavelength; [c]λ_{em} - emission wavelength; Φ_f - fluorescence quantum yield.

azo-N to Pd^{II} and significant charge delocalization from N-C_5H_4N-*m*/N-$C_5H_3N_2$-*o* fragment (ring-C) to the azo function intramolecularly.

Absorption and emission spectra :

The solution spectra of Pd(α/β-NaiR-N-C_5H_4N-*m*)Cl (**3**, **4**) and Pd(α/β-NaiR-N-$C_4H_3N_2$-*o*)Cl (**5**, **6**) in acetonitrile is entirely different from Pd(α/β-NaiR)Cl_2. The complexes **3-6** show multiple transitions in the visible to NIR region (450–850 nm). The acetonitrile solution of Pd(α/β-NaiR)Cl_2 exhibit absorption bands at 240–550 nm. The spectral data are collected in Table 2 and a representative figure is shown in Fig. 3. On comparison with the absorption spectra of the free ligand[18] we conclude that transitions <400 nm are intraligand charge transfer transitions. The transitions in visible to NIR region are characteristic to C–N fused system. We have attempted to explain the origin of these transitions from DFT computation data (*vide supra*).

The photoluminescence properties of the complexes **3-6** were studied at room temperature (298 K) in MeCN solution (Fig. 3). Pd(α/β-NaiR-N-C_5H_4N-*m*)Cl and Pd(α/β-NaiR-N-$C_4H_3N_2$-*o*)Cl exhibit emission at 340–450 nm (Table 2). The emission is assigned to the intraligand fluorescence (π-π* state). Longer wavelength (λ > 500 nm) excitation does not show emission[20].

The effect of solvent polarity on the absorption is insignificant while the fluorescence spectra of the complexes (**3-6**) show sufficient shifting of emission band when recorded in a series of non-hydroxylic and hydroxylic solvents. Fig. 4 shows emission behaviour of Pd(α-NaiEt-N-C_5H_4N-*m*)Cl in different solvents. Excitation is carried out at 253 nm. In general, the absorption band shifts to shorter wavelength with increasing solvent polarity which means better stabilization of ground state HOMO compared to LUMO with increasing polarity; while increase in solvent polarity shifts emission to longer wave-

Table 3. ^{1}H NMR spectral data of Pd(α/β-NaiR-N-C_5H_4N-*m*)Cl (**3**, **4**) and Pd(α/β-NaiR-N-$C_4H_3N_2$-*o*)Cl (**5**, **6**) in $CDCl_3$

Compd.	δ/ppm (*J*/Hz)										
	4-H[a]	5-H[a]	8-H[b]	9-H[b]	10–13-H[b]	15-H[c]	16-H[b]	17,18-H[b]	19-H[a]	N-CH_3[c]	N-CH_2	(N-CH_2)CH_3
3a	7.31	7.09	7.87(8.0)	7.80	7.65–7.75	8.80		8.06	8.15(7.0)	4.08		
3b	7.30	7.03	7.85(8.0)	7.51	7.65–7.75	8.77		8.06	8.18(8.0)		4.55[d](10.0)	1.48[e](8.0)
3c[f]	7.33	7.03	7.83(7.4)	7.79	7.65–7.75	8.65		8.05	8.16(8.0)		5.74[c]	
4a	7.35	7.08	7.82(7.1)	7.65	7.60–7.80	8.57		8.04	8.18(7.0)	4.06		
4b	7.30	7.09	7.81(7.5)	7.70	7.55–7.70	8.57		8.05	8.17(7.0)		4.50[d](10.0)	1.44[e](7.0)
4c[f]	7.34	7.06	7.80(8.0)	7.75	7.70–7.80	8.55		8.03	8.15(7.0)		5.72[c]	
5a	7.28	7.01	7.56(7.0)	7.78	7.54–7.72		8.01	8.00		4.02		
5b	7.31	7.00	7.53(7.0)	7.56	7.53–7.88		8.03	8.04			4.35[d](10.0)	1.44[e](8.0)
5c[f]	7.22	7.05	7.54(7.3)	7.33	7.56–7.65		8.00	8.02			5.76[c]	
6a	7.28	7.09	7.55(7.3)	7.31	7.52–7.77		8.04	8.07		4.00		
6b	7.25	7.01	7.52(7.0)	7.23	7.45–7.65		8.00	8.00			4.05[d](10.0)	1.40[e](8.0)
6c[f]	7.34	7.00	7.67(7.2)	7.33	7.56–7.73		8.01	8.01			4.00[c]	

[a]Doublet, [b]Multiplet, [c]Singlet, [d]Quartet, [e]Triplet, *f*δ(Ph) : 7.45–7.60 ppm.

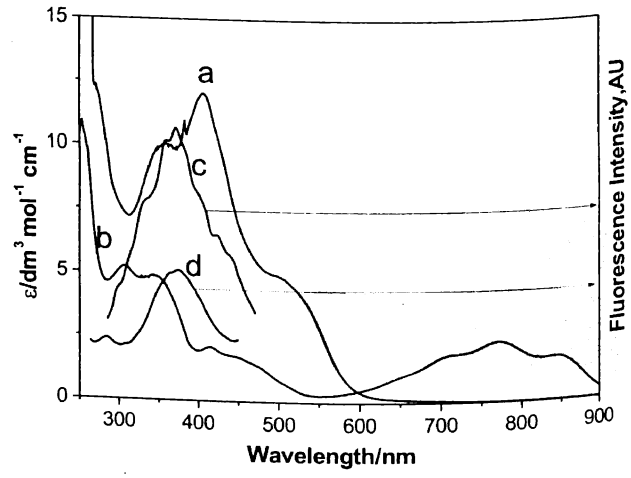

Fig. 3. Absorption spectra of (a) Pd(α-NaiEt)Cl_2, (b) Pd(α-NaiEt-N-C_5H_4N-*m*)Cl and fluorescence spectra of (c) Pd(α-NaiEt)Cl_2, (d) Pd(α-NaiEt-N-C_5H_4N-*m*)Cl in acetonitrile solution at room temperature.

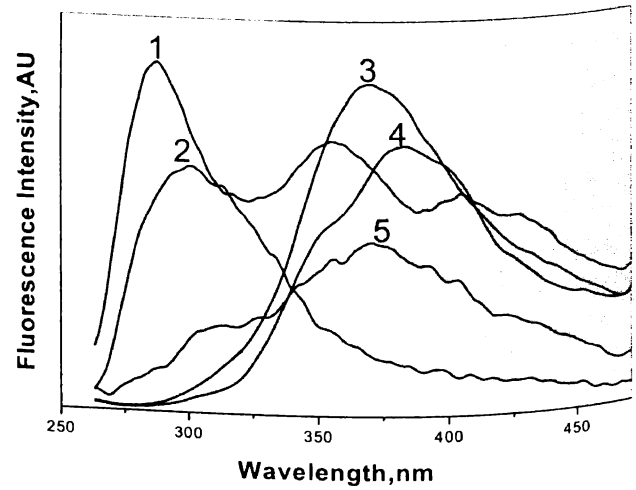

Fig. 4. Solvatochromic effect on fluorescence spectra of Pd(α-NaiEt-N-C_5H_4N-*m*)Cl in different solvents. *t*-BuOH (**1**), C_6H_6 (**2**), MeOH (**3**), CH_2Cl_2 (**4**), DMSO (**5**) solution at room temperature.

length : λ_{em}(solvent) : 383 ($CHCl_3$), 370 (DMSO), 385 (THF), 370 (MeOH), 380 (CH_2Cl_2), 374 (EtOH), 299 (C_6H_6), 372 (MeCN), 312 (ethyleneglycolmonomethyl ether), 354 (DMF), 296 (toluene), 357 (t-BuOH). This implies destabilization of HOMO upon excitation in more polar solvent than that of LUMO.

^{1}H NMR spectral characterisation :

The ^{1}H NMR spectra of Pd(α/β-NaiR-N-C_5H_4N-*m*)Cl (**3**, **4**) and Pd(α/β-NaiR-N-$C_4H_3N_2$-*o*)Cl (**5**, **6**) were recorded in $CDCl_3$ and the results are summarized in Table

3. The signals were compared with free ligand and Pd(α/β-NaiR)Cl_2 and have been assigned[15]. The imidazole-H (4 and 5-H) (A-ring) appear at 7.00 to 7.35 ppm. *m*-Pyridyl (C-ring) protons show singlet for15-H at 8.55–8.80 ppm, which is due to proximity of pyridine-N and metalated amine-N centre. Other protons (17-H and 18-H) appear at 8.00 to 8.10 ppm. β-Naphthyl shows (9-H to 13-H) protons at up-field region relative to *m*-pyridyl protons.

Electrochemistry :

The results of cyclic voltammetry of Pd(α/β-NaiR-N-C_5H_4N-*m*)Cl (**3**, **4**) and Pd(α/β-NaiR-N-$C_4H_3N_2$-*o*)Cl (**5**, **6**) are given in Table 4 and a representative voltammogram is shown in Fig. 5. Pd(β-NaiR)Cl_2 exhibit two quasireversible (ΔE_p > 100 mV) reduction couples at negative to SCE and have been assigned to reduction of azo group[13–15]. The complexes **3-6** show three successive redox couples. One redox couple appears at positive side to SCE in the potential range 0.8–1.2 V and is oxidative in nature. This redox response is quasirevesible in nature which is supported from $\Delta E_p \geq 100$ mV ($\Delta E_p = [E_{pa} - E_{pc}]$, peak-to-peak separation). One electron nature of the redox couple is supported from i_{pa}/i_{pc} (≈1.0) and differential pulse voltammetry (DPV). Palladium(II) is hard to oxidize, so this oxidative response is referred to the ligand oxidation at the easily oxidisable chelate ring 2, eq. (4). Because of better π-acidity of pyrimidine

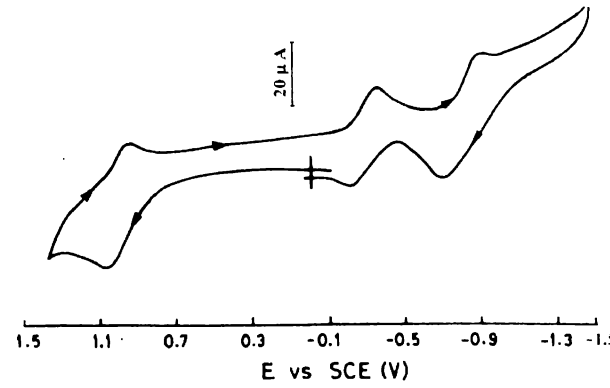

Fig. 5. Cyclic voltammogram of Pd(α-NaiEt-N-C_5H_4N-*m*)Cl (**3b**) in acetonitrile solution using Pt-working electrode, SCE reference and Pt-wire auxiliary electrode in presence of [n-Bu^t_4N](ClO_4) as supporting electrolyte.

base than pyridine the complexes **5** and **6** may show higher oxidation potential than the complexes **3** and **4** (Table 4). Two redox responses appear at negative to SCE at -0.2 to -0.3 and -0.7 to -0.9 V are reductive in nature. The reduction is regarded as the electron accommodation in the LUMO characterized by azoimine function. There are four successive redox accessible levels in -N=N-C=N- group. However, up to -1.5 V of electrochemical scales we found two quasireversible reductions that are defined in eqs. (5) and (6). Further accommodation of electrons as per eqs. (7) and (8) may experience strong electronic repulsion and may not be observable in the cyclicvoltammetric experiment within operating scale.

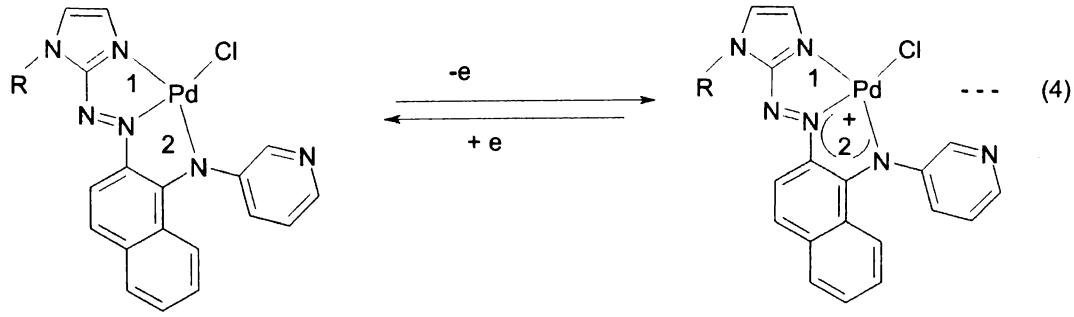

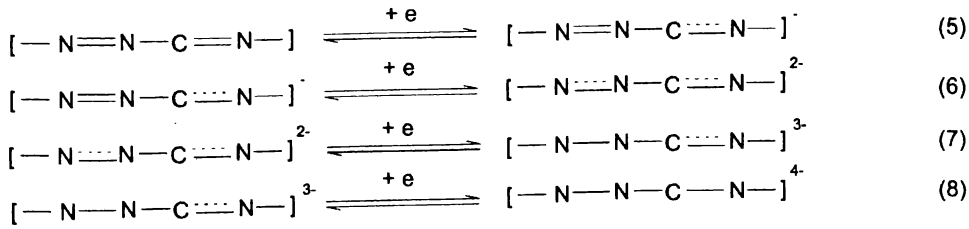

Table 4. Cyclic voltammetric data[a] of Pd(α/β-NaiR-N-C_5H_4N-*m*)Cl (**3**, **4**) and Pd(α/β-NaiR-N-$C_4H_3N_2$-*o*)Cl (**5**, **6**) in MeCN

Compd.	Oxidation	Reduction
	E/V (ΔE_p/mV)	-E/V (ΔE_p/mV)
3a	0.94(180)	-0.24(150), -0.82(180)
3b	1.01(180)	-0.23(170), -0.78(150)
3c	1.09(170)	-0.24(150), -0.80(130)
4a	0.92(180)	-0.29(140), -0.82(180)
4b	1.00(170)	-0.25(150), -0.83(190)
4c	1.05(160)	-0.25(140), -0.78(180)
5a	1.00(150)	-0.24(130), -0.81(160)
5b	1.08(170)	-0.22(150), -0.87(180)
5c	1.14(160)	-0.20(170), -0.82(170)
6a	1.02(180)	-0.22(180), -0.88(170)
6b	1.06(170)	-0.21(170), -0.78(175)
6c	1.19(180)	-0.20(160), -0.81(170)

[a]Solvent MeCN, Supporting electrolyte $[Bu_4N](ClO_4)$, Pt-disk milli working electrode, Pt-wire auxiliary electrode, Reference electrode SCE, at 298 K, E = 0.5 (E_{pa} + E_{pc}) where E_{pa} is anodic peak potential and E_{pc} is cathodic peak potential, ΔE_p = $|E_{pa} - E_{pc}|$; [b]E_{pc}. Scan rate - 100 mV/s.

DFT and TD-DFT calculation :

The optimized geometry of Pd(α-NaiEt-N-C_5H_4N-*m*)Cl (**3b**) is generated by using B3LYP-DFT calculations of G03 programme in solution phase (MeCN). The calculated structures well reproduce the experimental structures. The calculated Pd–N distances are about 0.01–0.03 Å longer than that of experimental data. The observed Pd–Cl distances are shorter by 0.01–0.02 Å than theoretical data. The orbital energies along with contributions from the ligands and metal are given in Table 5. Fig. 6 depicts the features of the selected occupied and unoccupied frontier orbitals. The energy difference between HOMO and LUMO, 2.26 eV is lower than the difference between HOMO-1 and LUMO, 3.22 eV. There are three significant parts in MOs : contribution from Pd, Cl and N,N′,N″-ligand. The chelated ligand N,N′,N″ has two parts : *m*-Pyridyl-N (N-Py-*m*), naphthylazoimidazole (α-NaiEt) units. The HOMO has 8% Pd, 27% N-Py-*m* and 65% α-NaiEt contribution. The HOMO-1 and HOMO-2 have major contribution from Cl (69% and 73% respectively). The LUMO is made up of 7% Pd, 12% N-Py-*m* and 79% α-NaiEt characters while LUMO+1 shares 47% Pd, 16% N-Py-*m* and 25% α-NaiEt and LUMO+2 has 92% α-NaiEt.

Table 5. Selected orbital energies and orbital compositions (%) for Pd(α-NaiEt-N-C_5H_4N-*m*)Cl (**3b**) in MeCN solution phase

MOs	E, eV	% Pd	% Amine	% α-NaiEt	% Cl
L+10	1.36	94	1	5	0
L+9	1.07	98	0	2	0
L+8	0.95	95	1	3	1
L+7	0.70	1	2	97	0
L+6	0.44	2	0	98	0
L+5	0.15	6	69	25	0
L+4	-0.48	2	31	67	0
L+3	-0.58	2	87	11	0
L+2	-1.09	1	7	92	0
L+1	-1.62	47	16	25	12
L	-3.06	7	12	79	2
H	-5.32	8	27	65	0
H-1	-6.28	21	0	10	69
H-2	-6.31	15	9	4	73
H-3	-6.54	2	23	74	1
H-4	-6.68	19	70	3	8
H-5	-6.89	53	27	16	3
H-6	-7.27	17	47	33	3
H-7	-7.29	16	0	75	8
H-8	-7.51	33	6	53	8
H-9	-7.54	8	21	40	31
H-10	-7.69	10	79	9	2

H = HOMO; H-1 = HOMO-1 etc. L = LUMO; L+1 = LUMO +1 etc.

To gain detailed insight into the charge transitions, the TD-DFT calculations were performed. Calculated absorption spectra of the complexes are shown in Fig. 7; theoretical excitation wavelength and their assignment are given in Table 6. Intense (oscillator strength *f*, 0.122) transition at 679 nm followed by a band at 411 nm (*f*, 0.136) are characteristics to HOMO→LUMO and HOMO-3→LUMO those are significantly ILCT (intraligand charge transfer) transitions. Two major transitions in UV region are at 329 (*f*, 0.187) and 291 (*f*, 0.192) mixture of ILCT and XLCT (X = Cl). The experimental spectra show structured absorption in visible to NIR region, 600–900 nm which is in agreement with the theoretically derived spectrum (Fig. 7).

Redox properties of the complexes are also corroborated by the electronic structure of the molecules. Oxidation is the electron abstraction from HOMO which is contributed ~92% from chelated ligand. Thus, the oxidation is ligand centred and description in eq. (2) is jus-

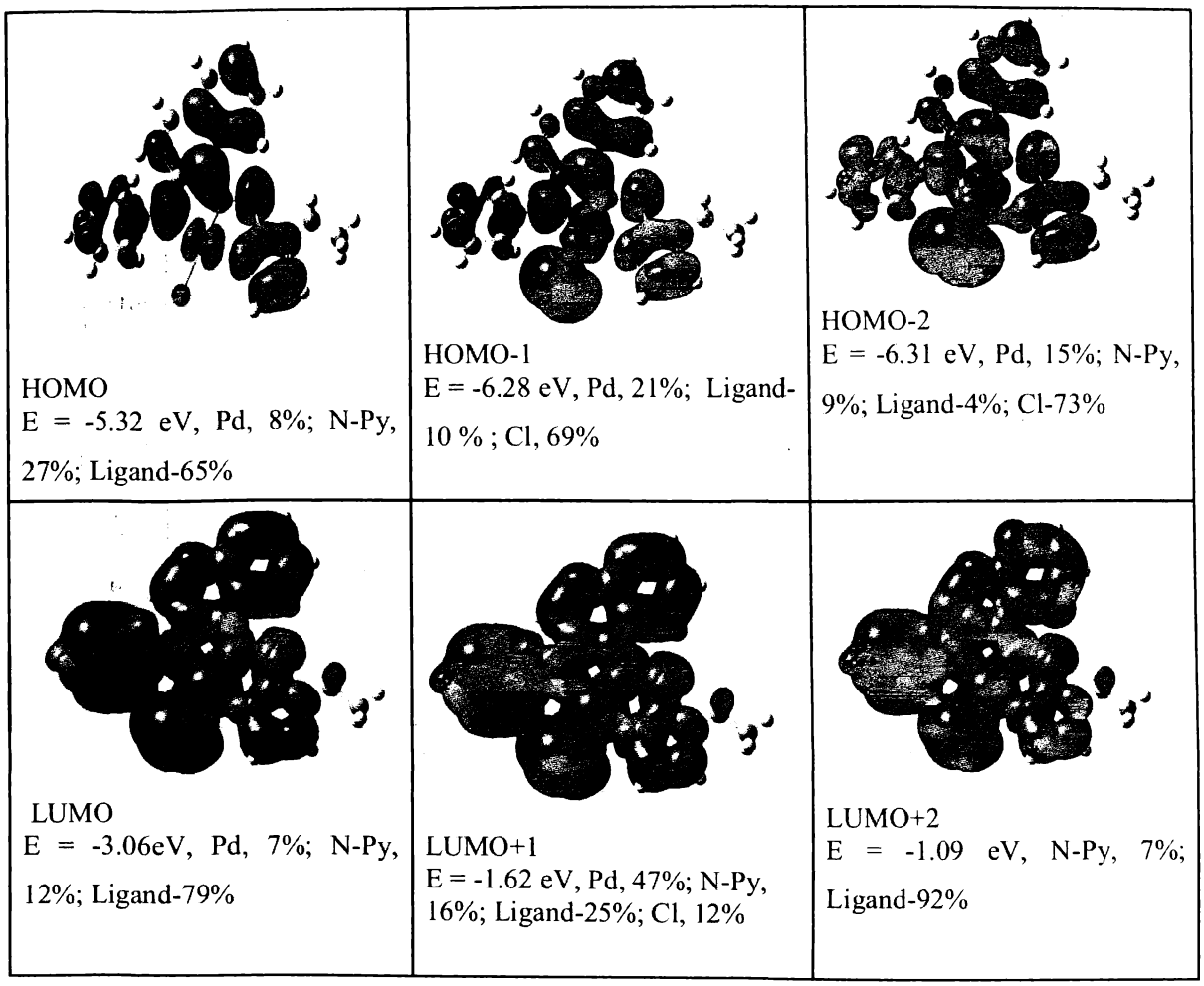

Fig. 6. Some selected molecular orbital pictures of Pd(α-NaiEt-N-C_5H_4N-*m*)Cl.

tified. The LUMO is also 91% from chelated ligand and thus reduction is also ligand centred.

Experimental

Materials : 1-Alkyl-2-(naphthyl-α/β-azo)imidazoles (α-NaiR and β-NaiR, R = CH_3 (**a**), CH_2CH_3 (**b**), CH_2Ph (**c**)) and Pd(α/β-NaiR)Cl_2 (α-NaiR (**1**), β-NaiR (**2**)) were prepared by reported procedure[15]. *m*-Aminopyridine and *o*-aminopyrimidine were received from Sisco Research Lab (SRL). The purification of acetonitrile and preparation of *n*-tetra butylammonium perchlorate [n-Bu_4N][ClO_4] for electrochemical work were done as before[12]. Dinitrogen was purified by bubbling through an alkaline pyrogallol solution. Solvents used for solvatochromic study were purified by reported procedure[17]. All other chemicals and solvents were of reagent grade and were used without further purification. Commercially available SRL silica gel (60–120 mesh) was used for column chromatography.

Measurements : Microanalytical data (C, H, N) were collected on Perkin-Elmer 2400 CHNS/O elemental analyzer. Spectroscopic data were obtained using the following instruments : UV-Vis spectra, Lambda 25, Perkin-Elmer; IR spectra (KBr disk, 4000–450 cm^{-1}), FTIR RX 1, Perkin-Elmer; ^1H NMR spectra, Bruker (AC) 300 MHz FTNMR spectrometer. Emission was examined by LS 55 Perkin-Elmer spectrofluorimeter at room temperature (298 K) in MeCN under degassed condition. Electrochemical measurements were performed using computer-controlled PAR model 270 VERSASTAT electrochemical instruments with Pt-disk electrodes. All measurements were carried

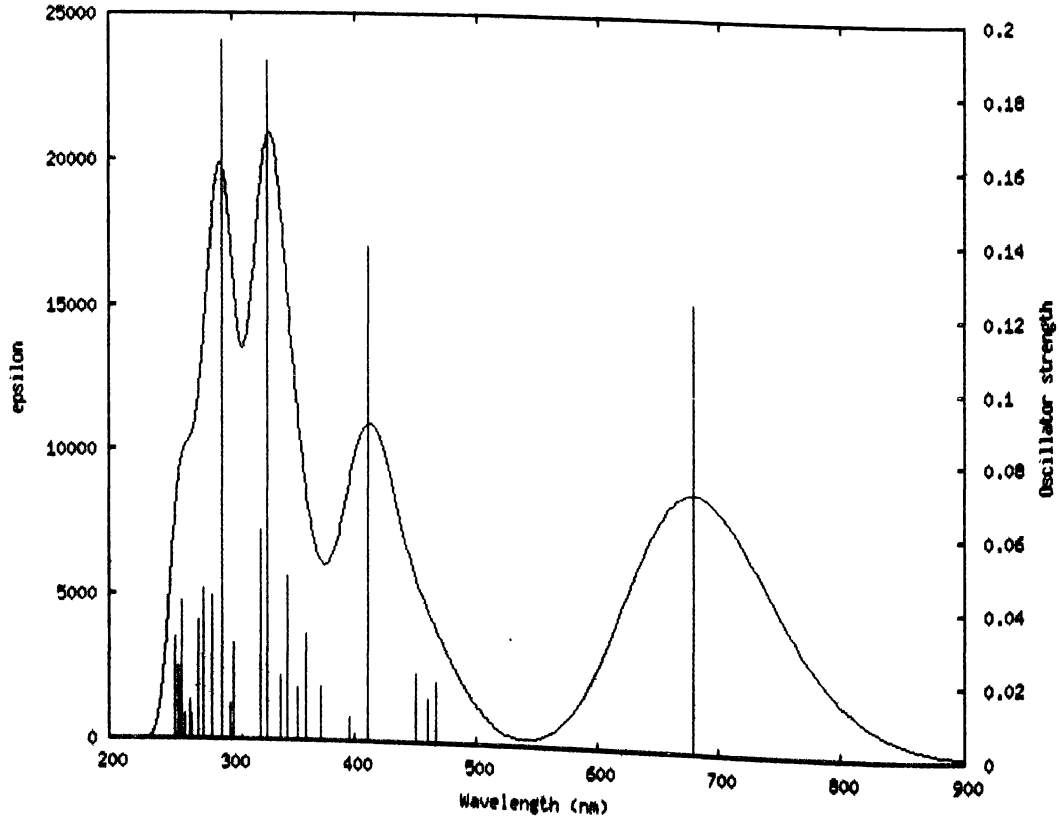

Fig. 7. Theoretically computed UV-Visible spectrum of Pd(α-NaiEt-N-C_5H_4N-*m*)Cl **(3b)**.

Table 6. Selected list of excited energies of Pd(α-NaiEt-N-C_5H_4N-*m*)Cl **(3b)** in acetonitrile phase

λ (nm)	Oscillator strength ($f \times 10^3$)	Major transitions	Assignment
679	0.1224	HOMO→LUMO(60%)	ILCT
411	0.136	H-3→LUMO(64%)	ILCT
361	0.0292	H-8→LUMO(27%)	ILCT(major)+MLCT
		H-6→LUMO(50%)	
345	0.045	H-7→LUMO(23%)	ILCT
		H-6→L+1(16%)	XLCT+ILCT
		H-5→L+1(41%)	MMCT
		H-4→L+1(30%)	XMCT
329	0.1868	HOMO→L+2(58%)	ILCT(major)+XLCT
		HOMO→L+4(19%)	ILCT(major)+XLCT
323	0.0577	H-8→LUMO(52%)	ILCT
		H-7→LUMO(33%)	ILCT
291	0.1924	HOMO→L+4(58%)	ILCT(major)+XLCT
284	0.0394	H-8→L+1(22%)	LMCT+MMCT
		H-3→L+1(37%)	LMCT+ILCT
		HOMO→L+4(23%)	ILCT
277	0.0417	H-7→L+1(10%)	LMCT(major)+ILCT
		H-4→L+1(44%)	XMCT

Table-6 (contd.)

259	0.0384	H-7→L+1(35%)	LMCT(major)+ILCT
		H-6→L+1(24%)	XLCT+ILCT
		HOMO→L+5(18%)	LXCT

(MLCT : Metal-to-ligand charge transfer; XMCT : Amine-to-metal charge transfer; XLCT : Ligand-to-ligand charge transfer; ILCT : Intraligand charge transfer; H = HOMO; L = LUMO).

Table 7. Crystallographic data of Pd(α-NaiEt-N-C_5H_4N-*m*)Cl (**3b**) and Pd(α-NaiMe-N-$C_4H_3N_2$-*o*)Cl (**5a**)

	3b	**5a**
Formula	$C_{20}H_{17}ClN_6Pd$	$C_{18}H_{14}ClN_7Pd$
Formula weight	483.25	470.21
Crystal colour	Green	Red
Crystal size (mm^3)	0.20 × 0.05 × 0.05	0.10 × 0.01 × 0.01
Crystal system	Monoclinic	Monoclinic
Space group	*P*2(1)/*c*	*P*2(1)/*n*
a (Å)	18.780(8)	14.592(4)
b (Å)	12.675(5)	14.193(3)
c (Å)	7.860(3)	17.802(3)
β (°)	90.229(7)	107.344(7)
V ($Å^3$)	1870.9(13)	3519.1(13)
Z	4	8
T (K)	93(2)	93(2)
λ (Å)	0.71073	0.71073
2θ range (°)	$5.4 \le 2\theta \le 50.72$	$3.18 \le 2\theta \le 50.66$
hkl range	$-21 \le h \le 22$,	$-14 \le h \le 17$,
	$-14 \le k \le 15$,	$-16 \le k \le 16$,
	$-9 \le l \le 9$	$-21 \le l \le 16$
ρ_{calc} (g cm^{-3})	1.716	1.775
μ (Mo Kα) (mm^{-1})	1.154	1.226
Reflection collected	18093	22498
Unique reflections	3413	3347
R^a	0.0743	0.0816
wR^b	0.1659	0.1492
Goodness-of-fit	1.150	1.003

$^aR_1 = \Sigma|F_o - F_c|/\Sigma F_o$. $^bwR_2 = [\Sigma w(F_o^2 - F_c^2)/\Sigma wF_o^4]^{1/2}$, $w = 1/[\sigma^2(F^2)+(0.0655P)^2 + 1.2687P]$ for (**3b**). $w = 1/[\sigma^2(F^2)+(0.0482P)^2 + 0.000P]$ for (**5a**).

out under a nitrogen environment at 298 K with reference to saturated calomel electrode (SCE) in acetonitrile using [n-Bu_4N][ClO_4] as supporting electrolyte. The reported potentials are uncorrected for junction potential.

Luminescence property was measured using LS-55 Perkin-Elmer fluorescence spectrophotometer at room temperature (298 K) in CH_3CN solution by 1 cm path length quartz cell. The fluorescence quantum yield of the complexes was determined using naphthalene laser dye as a reference with a known ϕ_R (fluorescence quantum yield of reference) of 0.21 in MeCN[18]. The complex and the reference dye were excited at 250–310 nm for Pd(α/β-NaiR-N-C_5H_4N-*m*)Cl and Pd(α/β-NaiR-N-$C_4H_3N_2$-*o*)Cl maintaining nearly equal absorbance (~0.1) and the emission spectra were recorded from 300–500 nm for **3-6**. The area of the emission spectrum was integrated using the software available in the instrument and the quantum yields were calculated according to the following equation :

$$\phi_S/\phi_R = [A_S/A_R] \times [(Abs)_R/(Abs)_S] \times [\eta_S^2/\eta_R^2]$$

Here ϕ_S and ϕ_R are the fluorescence quantum yield of the sample and the reference, respectively; A_S and A_R are the area under the fluorescence spectra of the sample and the reference respectively, $(Abs)_S$ and $(Abs)_R$ are the respective optical densities of the sample and the reference solution at the wavelength of excitation, and η_S and η_R are the values of refractive index for the respective solvent used for the sample and the reference.

***Preparation of complexes* :**

***Chloro[1-ethyl-2-{(7-imidopyridyl-m)naphthyl-α-azo}imidazole-N,N',N'']palladium(II), Pd(α-NaiEt-N-C_5H_4N-m)Cl,* (3b) :**

To an acetonitrile solution (20 ml) of Pd(α-NaiEt)Cl_2 (0.076 g, 0.18 mmol) was added slowly *m*-Py-NH_2 (0.025 g, 0.26 mmol) in the same solvent (10 ml). And 0.4 ml triethylamine was added to this solution. The reaction mixture was stirred and refluxed for 10 h. The colour of the solution changed gradually from orange-red to green. The solution was evaporated in air, and the residue was washed thoroughly first with water (2 × 5 ml) and then with 50% aqueous-ethanol (3 × 5 ml). The residue was dissolved in dichloromethane (10 ml) and the solution was chromatographed over silica gel column (60–120 mesh). A green band was eluted by MeCN. The eluted solution on evaporation in vacuo gave pure compound.

Green compound was isolated in 53% yield. This product is the coupled product, Pd(α-NaiEt-N-C_5H_4N-*m*)Cl (**3b**). A red band was also eluted by acetonitrile and had remained uncharacterized till date.

All other complexes were prepared similarly; yield, 45–55%. Calcd. for $C_{19}H_{15}N_6ClPd$ (**3a**) : C, 48.66; H, 3.20; N, 17.93. Found : C, 48.60; H, 3.19; N, 17.88%. Calcd. for $C_{20}H_{17}N_6ClPd$ (**3b**) : C, 49.74; H, 3.52; N, 17.41. Found : C, 49.66; H, 3.50; N, 17.39%. Calcd. for $C_{25}H_{19}N_6ClPd$ (**3c**) : C, 55.09; H, 3.49; N, 15.43. Found : C, 55.01; H, 3.44; N, 15.41%. Calcd. for $C_{19}H_{15}N_6ClPd$ (**4a**) : C, 48.66; H, 3.20; N, 17.93. Found : C, 48.62; H, 3.18; N, 17.85%. Calcd. for $C_{20}H_{17}N_6ClPd$ (**4b**) : C, 49.74; H, 3.52; N, 17.41. Found : C, 49.68; H, 3.51; N, 17.37%. Calcd. for $C_{25}H_{19}N_6ClPd$ (**4c**) : C, 55.09; H, 3.49; N, 15.43. Found : C, 55.03; H, 3.42; N, 15.40%. Calcd. for $C_{18}H_{14}N_7ClPd$ (**5a**) : C, 46.00; H, 2.98; N, 20.87. Found : C, 46.10; H, 2.99; N, 20.88%. Calcd. for $C_{20}H_{17}N_6ClPd$ (**5b**) : C, 47.15; H, 3.31; N, 20.27. Found : C, 47.16; H, 3.30; N, 20.29%. Calcd. for $C_{25}H_{19}N_6ClPd$ (**5c**) : C, 52.79; H, 3.29; N, 17.96. Found : C, 52.71; H, 3.24; N, 15.91%. Calcd. for $C_{19}H_{15}N_6ClPd$ (**6a**) : C, 46.00; H, 2.98; N, 20.87. Found : C, 46.02; H, 2.88; N, 20.85%. Calcd. for $C_{20}H_{17}N_6ClPd$ (**6b**) : C, 47.15; H, 3.31; N, 20.27. Found : C, 47.18; H, 3.33; N, 20.37%. Calcd. for $C_{25}H_{19}N_6ClPd$ (**6c**) : C, 52.79; H, 3.29; N, 17.96. Found : C, 52.73; H, 3.22; N, 17.90%.

X-Ray structure determination :

The X-ray quality single crystal of Pd(α-NaiEt-N-C_5H_4N-*m*)Cl (**3b**) (dimension 0.20 × 0.05 × 0.05 mm) and Pd(α-NaiMe-N-$C_4H_3N_2$-*o*)Cl (**5a**) (dimension 0.10 × 0.01 × 0.01 nm) were grown by slow diffusion of benzene into dichloromethane solution of the complex at 93(2) K. A summary of the crystallographic data and structure refinement parameters are given in Table 7. Data were collected with the Bruker SMART CCD using graphite-monochromatized MoKα radiation (λ = 0.71073 Å). Unit cell parameters were determined from least-squares refinement of setting angles with 2θ in the range $5.4 \le 2\theta \le 50.72^o$ of $-21 \le h \le 22$; $-14 \le k \le 15$; $-9 \le l \le 9$ for **3b** and $3.18 \le 2\theta \le 50.66$ of $-14 \le h \le 17$; $-16 \le k \le 16$; $-21 \le l \le 16$ for **5a**. Data were corrected for L_p effects and for linear decay. Semi-empirical absorption corrections based on multi-scans were applied. The structure was solved by direct method and refined by full-matrix least-squares refinement based on F_0^2 using SHELXL-97[19] and successive difference Fourier syntheses. Out of total reflections 18093 unique data were 3413 used for structure determination. Data reduction and refinement were carried out by Crystalclear of Rigaku Corporation using the programme of SHELEXL-97. All non-hydrogen atoms were refined anisotropically. The hydrogen atoms were fixed geometrically and refined using riding model. Hydrogen atoms were constrained to ride on the respective carbon or nitrogen atoms with an isotropic displacement parameters equal to 1.2 times the equivalent isotropic displacement of their parent atom in all cases. Maximum electron density is 0.842 and minimum electron density is -0.602. All calculations were carried out using SHELXL-97[19], ORTEP-32[20], PLATON-99[21].

Computational methods :

All computations were performed using the Gaussian03 (G03)[22] software package running under Windows. The Becke's three-parameter hybrid exchange functional and the Lee-Yang-Parr nonlocal correlation functional[23] (B3LYP) was used throughout. Elements except ruthenium were assigned a 6-31G* basis set in our calculations. For ruthenium the Los Alamos effective core potential plus double zeta (LanL2DZ)[24] basis set was employed. Gas and solution-phase optimization was carried out from the geometry obtained from the crystal structure without any symmetry constraints. In all cases, vibrational frequencies were calculated to ensure that optimised geometries represented local minima. The excitation energies were calculated by the TDDFT approach. To check the effect of solvation on the calculated optical absorption spectra, we performed TDDFT calculations of the low lying excitation at the singlet optimized geometry, including solvation effect by means of the nonequilibrium implementation of the polarizable continuum model[25]; as in the experimental conditions, the chosen solvent is acetonitrile. GaussSum[26] was used to calculate the fractional contributions of various groups to each molecular orbital. This is done using Mulliken population analysis.

Conclusion :

Pd(naphthylazoimidazole)Cl_2 have been reacted with 3-aminopyridine and 2-aminopyrimidine. The coupled products have been characterized by X-ray crystallography, other spectroscopic and electrochemical studies. The complexes are potentially fluorescent in solution. The emission process is dependent on polarity of the solvent. DFT calculation has determined electronic configuration and has explained the spectral and electrochemical properties.

Supplementary Information :

Crystallographic data for the structures of Pd(α-NaiEt-N-C_5H_4N-*m*)Cl (**3b**) and Pd(α-NaiMe-N-$C_4H_3N_2$-*o*)Cl (**5a**) have been deposited with the Cambridge Crystallographic Data Center, CCDC No. 844053 and 8445054 respectively. Copies of this information may be obtained free of charge from the Director, CCDC, 12 Union Road, Cambridge CB2 1EZ, UK (E-mail : deposit@ccdc.cam.ac.uk or www:htpp://www.ccdc.cam.ac.uk).

Acknowledgement

Financial supports from Department of Science and Technology and University Grants Commission (under CAS programme), New Delhi are thankfully acknowledged.

References

1. (a) B. K. Ghosh and A. Chakravorty, *Coord. Chem. Rev.*, 1989, **95**, 239; (b) A. Juris, V. Balzani, F. Bargelletti, S. Campagna, P. Belser and A. von Zelewsky, *Coord. Chem. Rev.*, 1988, **84**, 85; (c) A. H. Velders, H. Kooijman, A. L. Spek, J. G. Haasnoot, D. de Vos and J. Reedijk, *Inorg. Chem.*, 2001, **39**, 2966.
2. (a) R. Acharyya, S.-M. Peng, G.-H. Lee and S. Bhattacharya, *Inorg. Chem.*, 2003, **42**, 7378; (b) S. Nag, P. Gupta, R. J. Butcher and S. Bhattacharya, *Inorg. Chem.*, 2004, **43**, 4814; (c) P. Gupta, R. J. Butcher and S. Bhattacharya, *Inorg. Chem.*, 2003, **42**, 5405; (d) R. Acharyya, F. Basuli, R. Z. Wang, T. C. Mak and S. Bhattacharya, *Inorg. Chem.*, 2004, **43**, 704 and references therein; (e) C. Das, A. Saha, C. H. Hung, G.-H. Lee, S.-M. Peng and S. Goswami, *Inorg. Chem.*, 2003, **42**, 198.
3. (a) P. Byabartta, J. Dinda, P. K. Santra, C. Sinha, K. Panneerselvam, F. L. Liao and T. H. Lu, *J. Chem. Soc., Dalton Trans.*, 2001, 2825; (b) T. K. Misra, T. K. Das, C. Sinha, P. Ghosh and C. K. Pal, *Inorg. Chem.*, 1998, **37**, 167.
4. J. Pratihar, N. Maiti, P. Pattanayak and S. Chattopadhyay, *Polyhedron*, 2005, **24**, 1953.
5. M. Kurihara and H. Nishihara, *Coord. Chem. Rev.*, 2002, **226**, 125 and references therein.
6. (a) S. Chattopadhyay, C. Sinha, A. Basu and A. Chakravorty, *J. Organomet. Chem.*, 1991, **414**, 421; (b) S. Chattopadhyay, C. Sinha, A. Basu and A. Chakravorty, *Organometallics*, 1991, **10**, 1135 and references therein.
7. (a) K. K. Kamar, S. Das, C.-H. Hung, A. Castineiras, M. D. Kuzmin, C. Rillo, J. Bartolome and S. Goswami, *Inorg. Chem.* , 2003, **42**, 5367; (b) C. Das, S.-M. Peng, G.-H. Lee and S. Goswami, *New. J. Chem.*, 2002, **26**, 222; (c) P. Banerjee, G. Mostafa, A. Castineiras and S. Goswami, *Eur. J. Inorg. Chem.*, 2007, 412; (d) M. Panda, S. Das, G. Mostafa, A. Castineiras and S. Goswami, *Dalton Trans.*, 2005, 1249; (e) K. K. Kamar, P. Majumdar, A. Castineiras and S. Goswami, *Indian J. Chem., Sect. A*, 2003, **42**, 2320.
8. (a) P. K. Santra, P. Byabratta, S. Chattopadhyay, C. Sinha and L. R. Falvello, *Eur. J. Inorg. Chem.*, 2002, 1124; (b) S. Senapati, Sk. Jasimuddin, G. Mostafa, T.-H. Lu and C. Sinha, *Polyhedron*, 2006, **25**, 1571.
9. (a) C. K. Pal, S. Chattopadhyay, C. Sinha, D. Bandhyopadhyay and A. Chakravorty, *Polyhedron*, 1994, **113**, 999; (b) P. K. Santra, R. Roy and C. Sinha, *Proc. Indian Acad. Sci. (Chem. Sci.)*, 2000, **112**, 523.
10. B. K. Santra, P. Munshi, G. Das, P. Bharadwaj and G. K. Lahiri, *Polyhedron*, 1999, **18**, 617.
11. (a) U. S. Ray, D. Banerjee, G. Mostafa, T.-H. Lu and C. Sinha, *New. J. Chem.*, 2004, **28**, 1432; (b) D. Banerjee, U. S. Ray, Sk. Jasimuddin, J.-C. Liou, T.-H. Lu and C. Sinha, *Polyhedron*, 2006, **25**, 1299; (c) D. Banerjee, U. S. Ray, J.-C. Liou, C.-N. Lin, T.-H. Lu and C. Sinha, *Inorg. Chim. Acta*, 2005, **358**, 1019; (d) D. Banerjee, U. S. Ray, S. Chantrapromma, H.-K. Fun, J.-N. Lin, T.-H. Lu and C. Sinha, *Polyhedron*, 2005, **24**, 1071; (e) U. S. Ray, B. K. Ghosh, M. Monfort, J. Ribas, G. Mostafa, T.-H. Lu and C. Sinha, *Eur. J. Inorg. Chem.*, 2004, 250.
12. (a) D. Das, B. G. Chand, J. Dinda and C. Sinha, *Polyhedron*, 2007, **26**, 555; (c) B. G. Chand, U. Ray, J. Cheng, T.-H. Lu and C. Sinha, *Inorg. Chim. Acta*, 2005, **358**, 1927.
13. (a) J. Dinda, S. Pal, B. K. Ghosh, J. Cheng, F.-L. Liao, T.-H. Lu and C. Sinha, *J. Coord. Chem.*, 2002, **55**, 1271; (b) S. Senapati, U. S. Ray, P. K. Santra, C. Sinha, J. D. Woolins and A. M. Z. Slawin, *Polyhedron*, 2002, **21**, 753.

14. S. Pal, D. Das, C. Sinha and C. H. L. Kennard, *Inorg. Chim. Acta,* 2001, **313**, 21.

15. J. Dinda, P. K. Santra, C. Sinha and L. R. Falvello, *J. Organomet. Chem.*, 2001, **629**, 28.

16. P. Pratihar and C. Sinha, *J. Indian Chem. Soc.*, 2007, **84**, 623.

17. A. I. Vogel, A. R. Tatchell, B. S. Furnis and A. J. Hannaford, "Vogel's Textbook of Practical Organic Chemistry", 5th ed., Prentice Hall, 1996.

18. B. Valuer, "Molecular Fluorescence : Principles and Applications", Wiley-VCH, Weinheim, 2001.

19. G. M. Sheldrick, SHELXS-97, "Program for the Solution of Crystal Structure", University of Gottingen, Germany, 1997.

20. G. M. Sheldrick, SHELXL-97, "Program for the Refinement of Crystal Structure", University of Gottingen, Germany, 1997.

21. A. L. Spek, "PLATON, Molecular Geometry Program", University of Utrecht, The Netherlands, 1999.

22. M. J. Frisch, G. W. Trucks, H. B. Schlegel, P. M. W. Gill, B. G. Johnson, M. A. Robb, J. R. Cheeseman, T. A. Keith, G. A. Petersson, J. A. Montgomery, K. Raghavachari, M. A. Al-Laham, V. G. Zakrzewski, J. V. Ortiz, J. B. Foresman, J. Cioslowski, B. B. Stefanov, A. Nanayakkara, M. Challacombe, C. Y. Peng, P. Y. Ayala, W. Chen, M. W. Wong, J. L. Andres, E. S. Replogle, R. Gomperts, R. L. Martin, D. J. Fox, J. S. Binkley, D. J. Defrees, J. Baker, J. P. Stewart, M. Head-Gordon, C. Gonzalez and J. A. Pople, "Gaussian 98"; Gaussian, Inc., Pittsburgh, PA, 1998.

23. C. Lee, W. Yang and R. G. Parr, *Phys. Rev. (B)*, 1988, **37**, 785.

24. P. J. Hay and W. R. Wadt, *J. Chem. Phys.*, 1985, **82**, 270.

25. M. Cossi and V. J. Barone, *Chem. Phys.*, 2001, **115**, 4708.

26. N. M. O'Boyle and J. G. Vos, "GaussSum 1.0"; Dublin City University, Dublin, Ireland, 2005. Available from http://gausssum.sourceforge.net.

27. J. Dinda, K. Bag, C. Sinha, G. Mostafa and T.-H. Lu, *Polyhedron*, 2003, **22**, 1367.